Generalized Entering Coefficients: A Criterion
For Foam Stability Against Oil in Porous Media

Topical Report

By
V. Bergeron
M. E. Fagan
C. J. Radke

September 1993

University of California, Berkeley
Berkeley, California

DISCLAIMER

This report has been reproduced directly from the best available copy.

Available to DOE and DOE contractors from the Office of Scientific and Technical Information, P.O. Box 62, Oak Ridge, TN 37831; prices available from (615)576-8401, FTS 626-8401.

Available to the public from the National Technical Information Service, U.S. Department of Commerce, 5285 Port Royal Rd., Springfield, VA 22161.

Generalized Entering Coefficients: A Criterion for Foam
Stability Against Oil in Porous Media

Topical Report

By
V. Bergeron
M. E. Fagan
C. J. Radke

September 1993

MASTER

Table of Contents

Generalized Entering Coefficients: A Criterion for Foam Stability Against Oil in Porous Media

V.Bergeron, M.E. Fagan*, and C.J.Radke[†]
Earth Sciences Division of Lawrence Berkeley Laboratory and Department of Chemical Engineering, University of California, Berkeley, CA 94720

[†] author to whom correspondence should be addressed
* Currently at the University of Illinois, Urbana

ABSTRACT

The unique mobility-control properties of foam in porous media make it an attractive choice as an injection fluid for enhanced oil recovery. Unfortunately, in many cases oil has a major destabilizing effect on foam. Therefore, it is important to understand how oil destabilizes foam and what surfactant properties lead to increased stability against oil. To explain the stability of foam in porous media in the presence of oil, we generalize the ideas of spreading and entering behavior using Frumkin-Deryaguin wetting theory. This formulation overcomes the inherent deficiencies in the classical spreading and entering coefficients used to explain foam stability against oil. We find that oil-tolerant foam can be produced by making the oil surface "water wet".

To test our theoretical ideas, we measure foam-flow resistance through 45-70 μm glass beadpacks, surface and interfacial tensions, and disjoining pressure isotherms for foam and pseudoemulsion films for a variety of surfactant/oil systems. Most notably, we measure pseudoemulsion-film disjoining pressure isotherms for the first time and directly establish that pseudoemulsion film stability controls the stability of the foam in the systems we tested. Moreover, we demonstrate the correspondence between stable pseudoemulsion films, negative entering behavior, and oil-tolerant foams.

INTRODUCTION

Foam as drive fluid for enhanced oil recovery (EOR) has shown promise, particularly in steamflooding field applications (1-3). In addition, foam may be an effective barrier to gas coning in thin oil zones (4). The unique mobility-control properties (i.e., large flow resistance) of foam in porous media make it an attractive choice. However, even though foam shows potential for improving oil recovery, it is not widely used partly because crude oils destabilize most foams. When flowing foam in porous media coalesces into its two separate phases, liquid and gas, it no longer provides a large flow resistance and is ineffective for oil recovery. Foam must remain stable against oil, that is remain as a dispersion of gas in liquid, for EOR applications. Therefore, it is important to understand how oil destabilizes foam and how increased stability against oil might be achieved.

Figure 1 shows a highly schematic diagram of foam bubbles percolating past a portion of residual oil in a porous medium (5). The aqueous surfactant solution is indicated by light shading, the rock is represented by cross-hatching, and the oil is shown as dark shading. As a lamella (i.e., a gas-water-gas or foam film) flows by a water-wet sand grain, it deposits a thick water film between the gas and solid. Provided that the residual oil globules are also water wet, flowing lamellae can similarly deposit thick water films over exposed portions of the oil. This gas-water-oil film is coined a pseudoemulsion film (6). It is possible for the pseudoemulsion film to thin and break under the capillary-pressure suction in the Plateau border that terminates the film. In this case the oil may enter the gas-water interface and spread as a gas-oil-water film or simply terminate the lamella. Thus, the fate of the deposited pseudoemulsion film is crucial to how oil interacts with foam in porous media.

Although considerable experimental work has focused on the interactions between oil and foam in porous media, much of it is contradictory. Most studies correlate foam stability results against thermodynamic criteria for entering and/or spreading of oil droplets

1

at a bulk aqueous solution-gas interface. Definitive correlation between bulk oil spreading and foam stability in porous media is not found (5,7-10). For instance, some researchers find that spreading oils destabilize foam more than nonspreading oils (7-9). Conversely, others find just the opposite (10). Still others note no correlation between spreading and foam destabilization (5) or that spreading effects are secondary (6,11-16). One reason for the inapplicabilty of bulk spreading and entering coefficients is that they do not account for the porous medium. Recognizing this, Kuhlman (10) defined a geometry-dependent spreading coefficient. Unfortunately, Kuhlman's spreading coefficient still does not include two important features displayed in Figure 1: thin-liquid films and capillary-suction pressure. Nevertheless, there is evidence for oil-tolerant foams in systems which have negative entering coefficients that are based solely on the bulk values of the interfacial tensions (5-15). Clearly, it is resonable to expect that oil must first penetrate the gas-water interface in order to destroy foam (14,16,17)).

Several researchers focus directly on the stability of the pseudoemulsion films (5,6,10,14,15). Manlowe and Radke (5) demonstrate by observing pore-level events of foam flowing in the presence of residual oil that foam stability in etched-glass mircomodels is controlled by the aqueous pseudoemulsion films separating oil and gas. Likewise, by investigating injection of pregenerated foams into and foam generation in porous sandstones at residual oil saturation, Raterman finds that foam stability is controlled primarily by pseudoemulsion film stability (15). Previously, Kruglyakov (18) showed that the stability of bulk foams exposed to organic liquids also relies on the longevity of pseudoemulsion films. Moreover, Kruglyakov maintains that bulk water spreading on oil (i.e., nonentering system) is a necessary, but not sufficient condition, for pseudoemulsion-film stability. Water spreading on oil is equivalent to the aqueous phase completely wetting the oil, as pictured in Figure 1.

Schramm and Novosad (11,12) and Schramm, Turta, and Novosad (13) focus on emulsification of the oil. They define a dimensionless lamella number, Λ, that along with

2

bulk spreading and entering coefficients characterizes foam stability against oil in porous media. Small emulsified oil droplets penetrate a lamella to destroy it. A lamella number greater than unity indicates that oil droplets small enough to enter the foam lamella are produced by the suction pressure in the Plateau borders of the lamellae. Then, the entering and spreading behavior of the droplets at the gas-water interface of the lamellae controls the final outcome. They maintain that the most oil-stable foam corresponds to a low Λ and a large negative entering coefficient. However, like the classical spreading coefficient, the lamella number relies only on bulk measurements and also fails to correlate with foam stability in the presence of oil (4).

This work unifies the two approaches proposed to account for oil-foam interactions: spreading behavior and thin-film stability. We demonstrate the correspondence between stable pseudoemulsion films, negative entering coefficients, and oil-tolerant foams. Frumkin-Deryaguin wetting theory is applied to the problem of oil-foam interactions to discover that stable pseudoemulsion films are essential to maintain oil-tolerant foam. This prediction is then critically tested by comparing steady-state foam flow behavior in glass beadpacks at residual oil saturation with measured disjoining pressure isotherms for both foam and pseudoemulsion films along with bulk surface and interfacial tensions.

THEORY

Spreading and Entering Coefficients

Attempts to correlate spreading behavior to foam destruction by oil forms the basis for most of the work performed on oil-destabilization mechanisms. These studies are descendents of the work done by Robinson and Woods (19) and Ross (20) who investigated mechanisms for the rupture of liquid films by antifoaming agents. They used the classical definitions of the spreading and entering (i.e. rupture) coefficients first derived

3

by Harkins (21). For oil at a gas-water interface the classical spreading and entering coefficients take the following form;

Spreading Coefficient : $\qquad S_{o/w} = \sigma_{wg} - \sigma_{ow} - \sigma_{og}$, $\qquad\qquad$ (1)

Entering Coefficient : $\qquad E_{o/w} = \sigma_{wg} + \sigma_{ow} - \sigma_{og}$, $\qquad\qquad$ (2)

where σ_{ij} corresponds to the surface or interfacial tension, and the subscripts o, w and g signify oil, water, and gas respectively. These relationships are meant to indicate that for a positive $S_{o/w}$ oil spreads over the gas-water interface, while a positive $E_{o/w}$ implies that oil penetrates the gas-water interface from the aqueous side. As pointed out by Ross (22) the entering and spreading coefficients are related in the following way, $-E_{o/w} = S_{w/o}$. Hence, a nonentering oil is thermodynamically equivalent to water spreading on a gas-oil interface. This equivalence is illustrated pictorially in Figure 2. Equations 1 and 2 do not, however, consider the geometry of the system or the influence of thin-film forces, and, therefore, their application to any physical process in porous media is severely limited.

Generalized Spreading and Entering Coefficients

To generalize the ideas of spreading behavior and its relation to foam stability we adopt the theory developed by Frumkin (23) and Deryaguin (24) for wetting fluids on a solid substrate (see also Churaev (25) and Hirasaki (26)). The underlying principle of the Frumkin-Deryaguin framework is incorporation of thin-film forces to describe wetting behavior. These forces, commonly expressed by the disjoining pressure isotherm, account for the stability of thin-liquid films. Inclusion of the disjoining pressure into the spreading and entering coefficients leads to a more general picture of how spreading and entering relate to film stability, defines coefficients that take into account thin-film properties, and directly accounts for the porous medium through the capillary-suction pressure.

4

The disjoining pressure, Π, was first introduced by Deryaguin and Obuchov (27). It represents the excess pressure acting normal to a film interface which results from the overlap of molecular interactions between the interfacial layers. This pressure is a function of the film thickness and can be either postive (disjoining) or negative (conjoining). A schematic of a disjoining pressure isotherm for a typical ionic surfactant-stabilized liquid film is pictured in Figure 3. Here we also identify the three primary components of the disjoining pressure; electrostatic repulsion, Π_{el}, van der Waals attraction, Π_{vw}, and steric/hydration, Π_{s-h} forces. These components combine to produce the dark solid line that represents the shape of the disjoining pressure isotherm. It is important to note that thermodynamically stable films can exist only in negatively sloping regions of the isotherm (28). In Figure 3 the portion of the curve with a positive slope separates the isotherm into two stable regions, thick (~ 50 nm) common black films (CBF) and thinner (~ 4 nm) Newton black films (NBF). These designations are, however, somewhat restrictive because they only pretain to systems that give a net 180° optical phase shift due to reflections at the interfaces. Typically, asymmetric films (e.g. pseudoemulsion films) exhibit refractive index changes that produce a zero net phase shift. Hence, below approximately 50 nm these films produce white instead of black films. Therefore, we also designate pseudoemulsion films that produce behavior analogous to a CBF or NBF as common white films (CWF) or Newton white films (NWF). When the distinction between white and black is not necessary, we simply refer to the two different types of films as common films (CF) and Newton films (NF).

The dashed lines in Figure 3 labelled as P_{c1} and P_{c2} represent two different capillary pressures applied to the film. When the capillary pressure intersects the isotherm in the negative sloping regions a (meta) stable film will be formed at the corresponding thickness. Therefore, from Figure 3 we see that P_{c1} can produce two films with different equilibrium thicknesses (CF or NF) while only thin Newton films can exist at P_{c2}. At even higher capillary pressures rupture of the film is inevitable.

The key step required to include thin-film forces into the classical form of the spreading or entering coefficient is to adopt the film tension model of the duplex interface (29-33). Figure 4 illustrates this idea for a pseudoemulsion film generated by bringing an oil droplet in solution to the gas-water interface. The thin aqueous film separating the oil from the gas provides a barrier against oil entering the gas phase. The expanded region in Figure 4 depicted by the circle and dashed lines, illustrates more clearly the transition of the thick pseudoemulsion film to the bulk aqueous phase.

Thin-film forces are readily incorporated into a generalized entering coefficient by first replacing the oil-gas surface tension with the tension of the aqueous film (26):

$$E^g_{o/w} = \sigma_{wg} + \sigma_{ow} - \sigma_f \,, \tag{3}$$

where σ_f denotes the pseudoemulsion film tension, and the superscript g indicates the generalized form of the entering coefficient. Next, the film tension is written in terms of the disjoining pressure isotherm (29-33),

$$\sigma_f(h_o) = \sigma_{wg} + \sigma_{ow} + \int_{\Pi(h_\infty)=0}^{\Pi = \Pi(h_o)} h \, d\Pi \,, \tag{4}$$

where h_o is the equilibrium thickness of the thin film at a particular disjoining pressure and h_∞ corresponds to a thick film that is not influenced by disjoining forces (i.e., $\Pi(h_\infty) = 0$). Ivanov and Kralchevsky (34) derive a more general film-tension expression for curved films. However, when $h_o/R_f \ll 1$ (e.g. $h_o \sim 100$ nm, $R_f \sim 10$ µm, where R_f is the radius of curvature of the film) their result reduces to Equation 4. Substitution of Equation 4 into Equation 3 defines the generalized oil-water entering coefficient,

6

$$E_{o/w}^g = - \int_{\Pi(h_\infty)=0}^{\Pi = \Pi(h_o)} h \, d\Pi \quad . \tag{5}$$

Hirasaki (26) presents an analogous expression for the spreading coefficient of a liquid over a solid substrate. Equation 5 relates the generalized entering coefficient to the disjoining pressure isotherm and, therefore to pseudoemulsion film properties. More importantly, for pseudoemulsion films that are not highly curved at equilibrium, $\Pi(h_o) = P_c$ (5). Even when the films are curved the disjoining pressure (and hence the limits of integration in Equation 5) can be evaluated from the capillary pressure and the film curvature (5,34,35). Thus the geometry and wetting saturation of the porous medium are automatically incorporated into the generalized entering coefficient through the imposed capillary pressure.

Graphical representations of the generalized entering coefficient with a model form of the disjoining pressure isotherm serve to reinforce the relationship between thin-film forces and entering behavior. Figure 5 represents the graphical interpretation of Equation 5 for a plane-parallel pseudoemulsion film that has both CWF and NWF branches in the isotherm. We immediately see the role of the imposed capillary pressure, shown as dashed lines in the figure, as the upper integration limit in Equation 5. Once this limit is set, the generalized entering coefficient simply becomes the negative of the shaded area displayed in the figure. In other words, a net positive area defines the system as nonentering. At the P_c indicated in Figure 5(a,b), the film has two equilibrium thicknesses. As a result, the generalized entering coefficient has two values depending on whether the film thickness corresponds to the outer or inner stable branch of the isotherm. For the $\Pi(h)$ isotherm in Figure 5(a,b) the total shaded area for each case is positive, which means that the system is

7

nonentering at both thicknesses. Further, we see that all purely repulsive disjoining pressure isotherms correspond to nonentering systems while purely attractive isotherms produce entering behavior. Therefore, systems that have pseudoemulsion film isotherms with large repulsive CWF branchs display negative entering behavior, produce highly stable pseudoemulsion films, and therefore exhibit foam stability against oil.

It is possible for isotherms with two values of the generalized entering coefficient to have one value negative and the other positive. This is illustrated in Figure 6 with a $\Pi(h)$ isotherm that has a large negative well. When the film is on the CWF branch of the isotherm at the indicated capillary pressure, as shown in Figure 6 (a), the net enclosed area is positive and the generalized entering coefficient is negative. In this case the applied capillary pressure does not overcome the force barrier generated by the film, and the pseudoemulsion film remains stable. Nonetheless, if the film is on the inner (NWF) branch at the indicated capillary pressure, as shown in Figure 6 (b), the net enclosed area is negative and the generalized entering coefficient is positive. That is, the system is entering in spite of the fact that a moleculary-adsorbed thin-liquid film separates the oil phase from the gas-water interface. This ultrathin film of order several solvent molecular layers in thickness, can support a finite contact angle between the bulk aqueous phase and the molecularly adsorbed film (26). In this regard nonentering systems (i.e. $E < 0$) may be thought of as oil-gas surfaces that are completely "wet" by water (i.e. zero macroscopic contact angle (36)) while entering systems (i.e. $E > 0$) correspond to nonwetting oil-gas interfaces for which the aqueous phase forms a finite contact angle.

Unlike the generalized entering coefficient, the classical entering coefficient has only one value for a given system. It is strictly a function of bulk surface and interfacial tensions and is a subcase of the generalized entering coefficient. For equilibrated aqueous surfactant solution/oil/gas systems, the classical entering coefficient corresponds to a pseudoemulsion film on the inner branch of the disjoining pressure isotherm at zero P_c. Graphical illustrations of the classical entering coefficient are shown in Figures 5c and 6c.

It is apparent from a comparison of the shaded areas in Figures 5 and 6 that the classical and generalized entering coefficients are significantly different and that the classical entering coefficient can be safely applied only when near zero P_c conditions prevail. The advantage of formulating a generalized entering coefficient is that we explicitly include thin-film force barriers. Further we directly account for the complex nature of the porous medium, since the capillary pressure imposed on the film is determined by both the geometry of the medium and saturation of the phases within the medium. Further illustrations of the differences between the classical and general entering coefficients are discussed in detail elsewhere (37, 38).

Our ideas concerning stability of foam against oil in terms of the generalized entering coefficient and pseudoemulsion films are closely related to the concept of a limiting capillary pressure for foam in porous media proposed by Khatib, Hirasaki and Falls (39). These authors experimentally establish a limiting capillary pressure in beadpacks, above which foam in oil-free porous media rapidly coalesces. It has recently been shown that the limiting capillary pressure in porous media without oil present is close to the rupture pressure of single foam lamellae, as determined from their disjoining pressure isotherms (40). If the capillary pressure in the porous medium exceeds the rupture pressure of the lamellae, the foam coalesces and provides little flow resistance. Therefore, we argue that the limiting capillary pressure for foam stability in oil-laden porous media is close to the pressure that makes the generalized entering coefficient positive, thereby creating nonwater wet oil patches that destroy the foam. When an aqueous surfactant lamella encounters a nonwetting oil region, thick water films that protect the lamella are no longer present. At this point destruction of the individual foam lamella may occur by oil spreading, contact angle induced pinch-off, or pinning of the lamella at the oil surface (17,41). Similar reasoning likely explains the finding that foam-flow resistance in oil-wet media is poor (10). Apparently, thick wetting films are required for robust foam in porous media. To test the ideas presented above we measure and compare the disjoining pressure isotherms of

9

single foam and pseudoemulsion films, surface and interfacial tensions, and steady state pressure gradients of flowing foam in glass beadpacks with and without residual oil. The basic premise is that a highly stable pseudoemulsion CWF (at the imposed capillary pressures) corresponds to a negative generalized entering coefficient which, in turn, produces oil-tolerant foam.

EXPERIMENTAL

Materials

Two surfactants are used in this study: sodium dodecyl sulfate (SDS), Kodak, Electrophoresis Grade, Lot 912031C, a conventional anionic surfactant, and DuPont Zonyl FSK, Lot 23 6/87, a zwitterionic fluorinated betaine surfactant. Although Zonyl FSK is nonconventional, it serves as a model nonentering system when used with dodecane oil. Chemical formulae of the surfactants are shown in Table 1. They are used with no further purification. Surface tension measurements as a function of SDS concentration, via the Wilhelmy-plate technique at ambient temperature, reveal a shallow minimum around the critical micelle concentration indicating trace amounts of impurities. The Zonyl FSK is a commercial surfactant mixture; no attempts were made to characterize its purity. Analytical grade sodium chloride is supplied by Mallinckrodt. All solutions are prepared using distilled water that is purified further with a four stage Milli-Q™ reagent grade water system from Millipore®. The oils in this study are 1,2,3,4-tetrahydronaphthalene (tetralin), Aldrich 99%, and dodecane, Aldrich 99+%. These too are used with no further purification. Their chemical formulae are also listed in Table 1. Combinations of these surfactant solutions and oils provide us with a wide range of spreading and entering behaviour.

10

Surfactant and NaCl concentrations are 0.50 active weight% and 0.83 weight%, respectively. All solutions are well above the critical micelle concentration (CMC). Since it is well known that SDS in water hydrolyzes into dodecyl alcohol (42), we use solutions of exactly the same age in all of our experiments to permit a meaningful comparison. When working with equilibrated systems, surfactant solutions and oils are placed in contact with mild mixing for at least two days prior to experiments. Careful surface tension, interfacial tension, and disjoining-pressure measurements verify that equilibration is complete. No stable emulsions were produced, even with moderate agitation.

Porous-Medium Measurements

The experimental equipment used for the porous-medium experiments is shown in Figure 7. Jencon Scientific UK grade 18 (45-70 μm) soda-glass beads are packed in a 1-cm inner diameter Omnifit High Performance Heavy Duty Glass Chromatography Column that is 10 cm long. The permeability is 2.3 μm^2 and the porosity is 0.37. A freshly packed column with new beads is used for each experiment. The column is weighed continuously by a Mettler BB 2400 Balance so that liquid saturation can be determined. We also maintain about 590 kPa (85 psi) of backpressure at the exit of the column during all flow experiments.

Nitrogen gas passes through a 2-μm Nupro Filter and is regulated by a Brooks 5850 Series Mass Flow Controller. Surfactant solutions are supplied by an Isco High Pressure Metering Pump, and oil is supplied from a glass syringe driven by a Harvard syringe pump. The column pressure drop and total system pressure are measured with Validyne DP-15 Variable Reluctance Pressure Transducers and CD23 and CD12 Signal Demodulators. Their output is plotted on a Linear Chart Strip Recorder which is read to $\pm$ 0.5 % of the full scale value of the transducer plate. Further experimental details are presented elsewhere (37).

Once the column is prepared for an experiment by saturation with the aqueous surfactant solution, nitrogen and surfactant solution are co-injected into the beadpack. The foam quality is set at 90% and the total superficial velocity at 3.3 m/day, both reported at the column exit. The pressure drop across the column and the total system pressure are recorded continuously as a function of time. These data allow the pressure gradient to be calculated as a function of the number of pore volumes of gas and liquid injected into the column. Liquid effluent from the column is also collected during the foam experiments. This effluent is often cloudy with small amounts of oil-in-water emulsions. However, oil is not produced as a separate phase. Weight measurement of the columns provide information for determining liquid phase staurations.

We have not directly measured the capillary pressure in our beadpacks. However, based on the model of Falls et.al. (43) for the capillary pressure in homogeneous beadpacks, we estimate that P_c in our foam-flow experiments is of order 1 kPa. This value can then be used to approximate $E_{o/w}^g$ from the measured disjoining presure isotherms.

Figure 8 shows typical pressure-gradient traces as a function of the amount of gas and surfactant solution injected for three different systems. The squares represent a SDS solution with no residual oil in the beadpack, the triangles correspond to a SDS brine solution equilibrated with tetralin and in the prescence of residual oil, and the circles are for a tetralin-equilibrated SDS solution in contact with residual tetralin. The pressure traces in Figure 8 rise rapidly at the beginning and then plateau to a steady-state value. The rapid rise at the start indicates that foam is generated almost immediately upon injection of the gas and surfactant solution. A large steady-state pressure gradient (i.e, large flow resistance) indicates a highly stable foam, and vice versa. The steady pressure gradients for the SDS and SDS+NaCl against residual tetralin are extremely large compared to that of water flowing through the beadpack under identical conditions. The foams produce a pressure gradient of approximately 22 MPa/m, whereas water as a single phase produces a pressure gradient on the order of 0.02 MPa/m. On the other hand, the SDS solution against residual

12

tetralin generates a steady-state pressure gradient of about 0.7 MPa/m. Thus, addition of salt protects the SDS foam against destabilization by tetralin.

Visual observations during the initial part of the foam-flow experiments show that the stronger foams advance through the porous medium in a piston-like fashion and achieve a large pressure drop before the gas reaches the end of the beadpack. The weaker foams, however, advance unevenly through the porous medium, and fingers of gas usually break through at a low pressure drop. All of the foams reach steady state around 20 pore volumes, except SDS equilibrated with tetralin (no residual oil present) which exceeded the maximum pressure limit of our foam flow apparatus, 33 MPa/m, at about 20 pore volumes. Most of the experiments are run for 130 pore volumes, although some are sustained for as long as several hundred pore volumes.

Three types of foam experiments are included in this work. The first and most severe test is the steady pressure gradient of foam flowing through glass beadpacks in the presence of residual oil. The oil and surfactant solution for this test are always pre-equilibrated. This test is the most severe because it simultaneously measures the stability of both foam and pseudoemulsion films for oil-equilibrated surfactant solutions. Large steady-state pressure gradients indicate stable foam and pseudoemulsion films. If, however, the foam is destabilized by oil, as evidenced by a low pressure gradient, either the foam and/or the pseudoemulsion films must also be unstable. Additional experiments are required to isolate whether the foam is destabilized by solubilized oil and/or by breakup of pseudoemulsion films.

Foam-flow experiments with surfactant solution equilibrated with oil but without residual oil in the beadpack are the second level of testing. They solely test the stability of foam films to solubilized oil. When solubilized-oil foam is stable without residual oil, but unstable in the presence of residual oil, the pseudoemulsion films provided by the presence of residual oil globules must be the culprit. If, however, the oil-equilibrated foam is also

unstable, both the foam and pseudoemulsion films may be unstable. Although possible, this scenario was not observed in our chemical systems.

The last and most simple test, is the flow of foam stabilized by surfactant solution. No oil equilibration, or residual oil contact is involved. This experiment strictly measures the foaming ability of the surfactant solution and is useful to determine the comparative effect that oil equilibration and the presence of residual oil have on the stability of the foam.

An implicit assumption behind these tests is that the gas-water-solid films are stable and do not contribute to the destabilization of flowing foam. We base this premise on observations that our glass beadpacks are strongly water wet even in the presence of oil and surfactant solution.

Disjoining Pressure Measurements

The experimental cell used to measure the disjoining pressure isotherms is depicted in Figure 9. This cell is a variant of the porous plate method developed by Mysels and Jones (44) and Exerowa and Scheludko (45). The individual films are formed in a 2-mm hole bored through a 1-cm diameter porous glass frit. The geometry of this hole is designed so that a range of capillary pressures can be applied to the film while maintaining a plane-parallel configuration (38). The cell can be used to investigate both, foam and pseudoemulsion films. Light shading in Figure 9 corresponds to the surfactant solution under investigation; pseudoemulsion films require an oil phase which is represented by dark shading. The entire cell is outfitted with a temperature control jacket and mounted on a vibration isolation table (StableTop TXT series). Using a micrometer-driven syringe pump we are able to regulate the gas pressure, P_g, in the cell. Manipulation of the cell pressure alters the imposed capillary pressure on the film, P_c, defined as $P_g - P_w$, where P_w is the liquid pressure in the Plateau-border region. At equilibrium, the capillary pressure applied

to the plane parallel portion of the film equals the disjoining pressure, Π, and is measured directly with a sensitive pressure transducer (Omega Model 750 DI).

A specially equipped reflected-light microscope permits film thickness measurements according to the thin-film interference technique developed by Scheludko and Platikanov (46). We use heat-filtered white light from an Oriel 200-W Hg-Xe Arc lamp to illuminate the films at zero angle of incidence. Independent verification of the film thickness, h_o, is provided by two different wavelengths of light (i.e. 546 nm and 665 nm) that are monitored simultaneously with thermoelectrically cooled photomultiplier tubes (Products for Research Model TE-104, RCA C3103402). After applying the standard Duyvis optical correction for adsorbed surfactant layers (48), our independent measurements of thickness agree to within $\pm$ 0.8 nm.

Disjoining pressure isotherms are generated by regulating the capillary pressure through adjustments in the gas pressure while simultaneously monitoring the film thickness. This process is aided by visual observations made from a video camera (Panasonic Digital 5000) attached to the microscope. Once the films reach equilibrium, the intensity of reflected light (to evaluate film thickness) along with the gas pressure are recorded. By gradually increasing and decreasing the gas pressure we map out the entire disjoining pressure isotherm. Additional experimental details are available elsewhere (38,47).

Surface and Interfacial Tension Measurements

Surface and interfacial tensions reported here are obtained with the drop-weight method. However, as a check, some surface and interfacial tensions were also measured with the Wilhelmy-plate (Roller-Smith Precision Balance by Biolar Corp.) and spinning-drop methods (University of Texas Spinning Drop Interfacial Tensiometer Model 300), respectively. Comparison of the data from each method shows that the tensions are accurate and that the agreement between methods is excellent (37). These techniques allow us to

determine classical entering and spreading coefficients accurate to ± 0.9 mN/m. In addition, visual observations were made of drops either placed onto or released from underneath surfactant solutions to confirm the predicted entering or spreading behavior.

RESULTS

Disjoining pressure isotherms, $\Pi(h)$, for foam (open symbols) and pseudoemulsion (solid symbols) films are shown on a semilogarithmic scale in Figures 10 to 13. The corresponding steady-state pressure gradients for flowing foam in glass beadpacks at 30 pore volumes of injected fluids are displayed on the figures and tabulated along with residual oil saturations in Table 2. Subscripts "f" and "or" on the pressure gradients listed in the figures indicate foam and foam against residual oil, respectively. Also, the pertinent surface and interfacial tensions, with the classical entering and spreading coefficients are presented in Table 3.

Figure 10 portrays the disjoining pressure isotherms for dodecane-equilibrated-SDS solution foam films and for SDS/dodecane pseudoemulsion films. It is clear that the foam film is considerably more robust than the pseudoemulsion film. The disjoining pressure isotherm for the foam film, shown as open diamonds, is much higher than the pseudoemulsion film disjoining pressure, shown as closed diamonds. Both films correspond to the outer branch (CF) of the schematic isotherm shown in Figure 3. The foam-film disjoining-pressure data continue as high as $\Pi=P_c=15$ kPa, with no rupture observed, which is the limit of our experimental apparatus for this system.

The pseudoemulsion film disjoining pressure in Figure 10 is significantly weaker than the foam film. The pseudoemulsion film ruptures near 0.1 kPa, which is several orders of magnitude below the highest disjoining pressure measured for the foam film. This indicates that either there is no inner branch (NWF) to this isotherm (i.e., purely

attractive forces dominate to zero thickness) or that there is at most a molecularly adsorbed layer that is below our thickness resolution.

The steady pressure gradient of dodecane-equilibrated SDS foam flowing in glass beadpacks is 6.1 MPa/m. With residual oil present the gradient is 0.12 MPa/m. Clearly, residual oil strongly destabilizes this foam. We also note that the residual oil saturation and classical entering coefficient listed in Tables 2 and 3 for SDS and dodecane are 25% and 22.4 mN/m (i.e., strongly entering), respectively. The entering coefficients in Table 3 agree with visual observations of submerged-oil-drop experiments.

Figure 11 is similar to Figure 10, except now for a SDS and tetralin system. Once again the pseudoemulsion film is much weaker than the foam film. The pseudoemulsion film ruptures near 0.2 kPa while the foam disjoining pressure continues through 15 kPa. Again, either there is no inner branch to the pseudoemulsion film isotherm or there is a molecularly adsorbed water layer at h=0.

For SDS, the steady-state pressure gradient is much lower with residual tetralin than without. The steady-state pressure gradient for SDS equilibrated with tetralin is greater than 33 MPa/m, which is the limit of our experimental apparatus. In the presence of residual tetralin the pressure gradient is 0.70 MPa/m. The classical entering coefficient for SDS and tetralin is again positive at 3.3 mN/m, and the residual oil saturation is 10%.

Figure 12 shows the disjoining pressure isotherms for Zonyl FSK foam and Zonyl FSK/dodecane pseudoemulsion films. This system is significantly different than the preceding two. Both films show high repulsive disjoining pressures and are stable beyond approximately 1.2 kPa. Neither film ruptures before the highest obtainable capillary pressure is reached in our experimental cell. Both disjoining pressure isotherms evidence highly stable CF branches.

The steady pressure gradient for Zonyl FSK against 29% residual dodecane is 22 MPa/m versus 19 MPa/m without residual oil or oil equilibration. This indicates that dodecane does not destabilize Zonyl FSK foam. Significantly, the classical entering

coefficient for this system is negative at -0.2 mN/m (i.e., nonentering). Again, visual observations of a dodecane drop released under a Zonyl FSK solution confirm that the oil is nonentering. Moreover, a dodecane drop placed gently on the Zonyl FSK solution surface is immediately engulfed and remains underwater.

Figure 13 is another example of highly repulsive foam and pseudoemulsion film disjoining pressures. The SDS+NaCl foam film is very strong. Its disjoining pressure continues beyond 12 kPa along an outer CBF branch. The pseudoemulsion film is also tough, with a rupture pressure of about 1 kPa. Again, with our technique, there is no evidence of an inner branch for the pseudoemulsion film. In glass beadpacks SDS with NaCl in the presence of residual tetralin produces a steady-state pressure gradient of 20 MPa/m, the same value obtained with no residual oil or oil equilibration. Interestingly, the addition of 0.83 wt% salt to a SDS solution reduces the classical entering coefficient, to -4.3 mN/m (i.e. highly nonentering). Visual observations confirm this result.

Figure 14 compares measured disjoining pressure isotherms for foam films of SDS solutions with and without oil equilibration. All of the foam films possess highly repulsive outer-branch disjoining pressures (CBF), exceeding 12 kPa, and no rupture is observed up to the limit of our apparatus. However, if we impose macroscopic disturbances on the films by rapidly increasing the capillary pressure, the oil-equilibrated films appear to break somewhat easier than the nonequilibrated films.

Steady pressure gradients for most of the systems in Figure 14 are listed in Table 3. Except for the SDS solution equilibrated with dodecane these data indicate that solubilized oil does not destabilize the foam tested in this study. Solubilization of dodecane reduces the steady-state pressure gradient by a factor of 4. Nonetheless, |ΔP|/L is still very large, and much greater than when residual oil is present. In addition, the steady-state pressure gradients for Zonyl FSK and SDS+NaCl without oil equilibration are equal to their values against residual oil.

18

DISCUSSION

Figures 10 through 13 and Table 3 show that systems with highly repulsive outer branches of the pseudoemulsion film disjoining pressure isotherms produce foam with large steady-state pressure gradients while flowing through glass beadpacks in the presence of residual oil. From Figures 10 and 11 we see that weak pseudoemulsion-film disjoining pressures correspond to low foam-flow resistances in the presence of residual oil. However, the surfactant formulations in Figures 12 and 13 display strong pseudoemulsion film disjoining pressures which correlate with large flow resistance in the presence of residual oil. It is apparent that for these four systems, pseudoemulsion-film stability controls the stability of flowing foam in oil-laden porous media. In otherwords, water wet oil surfaces (i.e., negative generalized entering systems) do not disrupt foam flow in porous media.

Earlier we discussed the concept of a limiting capillary pressure for pseudoemulsion films in porous media. The estimated 1 kPa capillary pressure in our glass beadpacks demands that pseudoemulsion films which cannot support pressures of this magnitude will rupture. Figures 10 and 11 evidence films that fall into this category. The pseudoemulsion-film rupture pressures are at or below 0.2 kPa and the foams for these systems are unstable to oil. Conversly, Figures 12 and 13 show pseudoemulsion films that are stable or do not rupture until the capillary pressure exceeds 1 kPa. Oil tolerant foams are observed in our beadpacks for these systems. Therefore, the limiting capillary pressure for the unstable cases appears to be between 0.2 and 1 kPa.

If we set the average capillary pressure applied to the pseudoemulsion films at 1 kPa, we can determine the sign of the generalized oil-water entering coefficients from the measured pseudoemulsion-film disjoining pressure isotherms and Equation 5. For Zonyl FSK/dodecane and SDS+NaCl/tetralin pseudoemulsion films, shown in Figures 12 and 13, the generalized entering coefficients are -0.02 mN/m and -0.01 mN/m, respectively,

19

corresponding to repulsive disjoining pressure isotherms. Direct evaluation of $E^g_{o/w}$ is possible for these films because the entire isotherm is available over the limits of intergration required in Equation 5 (i.e., no negative portion of the disjoining pressure isotherm exists between $\Pi(h_\infty) = 0$ and $\Pi(h_0) = P_c$). Unfortunately, we can only speculate that the generalized entering coefficients for SDS pseudoemulsion films against dodecane and tetralin are positive, because we cannot measure the negative region of Π that is required to quantify $E^g_{o/w}$ for these systems.

For the limited number of surfactant systems studied here the steady pressure gradients against residual oil correlate with both the generalized and classical entering coefficients (see Tables 2 and 3). Systems with negative classical entering coefficients exhibit larger flow resistances than those with positive entering coefficients. However, the classical form of the coefficients is at best a heuristic analysis as it neglects much of the relevant physics of the porous medium and thin films. Clearly, thin-film forces can generate force barriers that produce stable pseudoemulsion films (i.e., water-wet oil) in systems that show positive classical entering coefficients, depending on the capillary pressure exerted by the Plateau borders. In this case only the generalized form of the coefficients can predict the correct behavior.

Lamella numbers for our systems and the degree of foam stability to residual oil are shown in Table 4. Our results do not agree with the behavior predicted by Λ; that foam stability to oil in porous media increases for small values of Λ. The two stable systems in our work produce the lowest and highest lamella numbers, and the unstable systems fall in between. The most notable counter example is the SDS+NaCl against residual tetralin, which has the largest Λ and is highly stable. We believe that the lamella number theory is incomplete.

20

CONCLUSIONS

Previous work on destabilization of foam by oil has been approached in two seemingly different ways: spreading behavior and thin-film stability. Here we unify these concepts and demonstrate the inherent deficiency in the classical coefficients used to correlate foam stability correlations. Classical coefficients strictly apply only to zero P_C (applied capillary pressure), and they ignore thin-film force barriers. Since porous media exert rather large capillary pressures on liquid lamellae, this severly limits the predictive utility of the classical spreading parameters. When thin-film forces are included into a generalized entering coefficient, the zero-P_C restriction is eliminated, and the energetics of spreading or entering is naturally linked to film stability.

We find that oil-tolerant foam in porous media can be produced by making the oil surface "water wet" (i.e. zero contact angle). Highly stable pseudoemulsion films lead to negative values of the generalized entering coefficient and to thick aqueous wetting films covering the oil. Of course, the foam lamellae must also be independently stable at the capillary pressure imposed by the porous medium. If the capillary pressure reaches a threshold value, large enough to rupture the thick CW pseudoemulsion films and create a finite contact angle between the foam lamellae and the oil-gas surface or allow the oil to spread onto lamellae surfaces, then the oil can rupture the lamellae and destroy the foam.

Measurements of foam-flow resistance through glass beadpacks, surface and interfacial tensions, and disjoining pressure isotherms for foam and pseudoemulsion films, critically test our theoretical ideas. Most notably, we measure pseudoemulsion-film disjoining pressure isotherms for the first time and directly show that pseudoemulsion-film stability controls the stability of the foam in porous media for the systems we tested. Our results also indicate that a negative value of the generalized entering coefficient implies stable pseudoemulsion films, and hence oil-tolerant foam.

NOMENCLATURE

h	Film thickness, nm
h_o	Equilibrium film thickness, nm
h_∞	Film thickness at which $\Pi = 0$
L	length, m
Λ	Lamella number, dimensionless
P_c	Capillary pressure, kPa $(P_c = P_g - P_w)$
ΔP	Pressure difference, MPa
Π	Disjoining pressure, kPa
S	Saturation, dimensionless
σ	Equilibrated surface tension, mN/m

Subscripts

c	capillary
el	electrostatic repulsion forces
f	foam
g	gas
o	oil
or	residual oil
s-h	steric / hydration forces
vw	van der Waals forces
w	water

Superscripts

g	generalized

23

REFERENCES

1) Holm, L.W., "Foam Injection Test in the Siggins Field, Illinois," *JPT*, **22**, No. 12, 1499-1506 (1970).

2) Mohammadi, S.S., Slyke, D.C., and Ganong, B., "Steam-Foam Pilot Project in Dome-Tumbador, Midway-Sunset Field," *SPERE*, **4**, No. 1, 7-16 (1989).

3) Patzek, T.J., and Koinis, M.T., "Kern River Steam-Foam Pilots," *JPT*, **42**, No. 4, 496-503 (1990).

4) Hanssen, J.E., Rolfsvåg, T.A., Corneliussen, R., and Dalland, M., "Foam Barriers Against Gas Coning in Thin Oil Zones," paper presented at 5th European Symp. on Improved Oil Recovery, Budapest, Hungary (1989).

5) Manlowe, D.J., and Radke, C. J., "A Pore Level Investigation of Foam/Oil Interactions in Porous Media," *SPERE*, **5**, No. 4, 495-502 (1990).

6) Nikolov, A.D., Wasan, D.T., Huang, D.D., and Edwards, D.A., "The Effect of Oil on Foam Stability: Mechanisms and Implications for Oil Displacement by Foam in Porous Media," SPE paper 15443, presented at 61st Annual Tech. and Exhibition of the SPE, New Orleans, LA, 1-16 (1986).

7) Lau, H.C., and O'Brien, S.M., "Effects of Spreading and Nonspreading Oils on Foam Propagation Through Porous Media," *SPERE*, **3**, No.3, 893-896 (1988).

8) Kristiansen, T.S., and Holt, T., "Properties of Flowing Foam in Porous Media Containing Oil," preprint, SPE 8th Symp. on Enhanced Oil Recovery, Tulsa, Oklahoma, April 22-24, SPE paper 24182, 279-287 (1992).

9) Holt, T., and Kristiansen, T.S., "Improved Sweep Efficiency During Gas Injection - Mobility Control", Summaries of papers for the SPOR-Seminar, NPD, Stavanger, 59-77 (1990).

10) Kuhlman, M.I., "Visualizing the Effect of Light Oil on CO2 Foams," *JPT*, **42**, No. 7, 902-908 (1990).

11) Schramm, L.L., and Novosad, J.J., "Micro-Visualization of Foam Interactions with a Crude Oil," *Colloids and Surfaces*, **46**, 21-43 (1990).

12) Schramm, L.L., and Novosad, J.J., "The Destabilization of Foams For Improved Oil Recovery by Crude Oils: Effect of the Nature of the Oil," paper prepared for the Sixth European Symposium on Improved Oil Recovery held in Stavanger, Norway, May 21-23, 1991.

13) Schramm, L.L., Turta, A.T., and Novosad, J.J., "Microvisual and Coreflood Studies of Foam Interactions With a Light Crude Oil," preprint, SPE 7th Symp. on Enhanced Oil Recovery, Tulsa, Oklahoma, April 22-25, SPE paper 20197, 249-258 (1990).

14) Wasan, D.T., Nikolov, A.D., Huang, D.D., and Edwards, D.A., "Foam Stability: Effects of Oil and Film Stratification," in Surfactant Based Mobility Control - Progress in Miscible-Flood Enhanced Oil Recovery, ed. Smith, D.H., ACS Symp. Series 373, American Chemical Society, Washington D.C., Chapter 7, 136-162 (1988).

15) Raterman, K.T., "An Investigation of Oil Destabilization of Nitrogen Foams in Porous Media," preprint SPE 64th Annual Tech. Mtg., San Antonio, TX, 645-654 (1989).

16) Koczo, K., Lobo,L.A., and Wasan, D.T., " Effect of Oil on Foam Stability: Aqueous Foams Stabilized by Emulsions", *J. Colloid Int. Sci.*, **150**, No.2, 492-506, 1992.

17) Frye, G.C., "Interactions Between Surface Active Components in the Promotion and Destruction of Foams," Ph.D. Dissertation, Univ. of Washington (1987).

18) Kruglyakov, P.A., "Equilibrium Properties of Free Films and Stability of Foams and Emulsions," in Thin Liquid Films - Fundamentals and Applications, ed. Ivanov, I.B., Marcel Dekker Inc., New York, Chapter 11, 767-827 (1988).

19) Robinson, J.V., and Woods, W.W., "A Method of Selecting Foam Inhibitors," *J. Soc. Chem. Ind.*, **67**, 361-364 (1948).

20) Ross, S., "Inhibition of Foaming. II A Mechanism for the Rupture of Liquid Films by Antifoaming Agents," *Chem. Eng. Prog.*, **54**, 429-436 (1950).

21) Harkins, W.D., "A General Thermodynamic Theory of the Spreading of Liquids to Form Duplex Films and of Liquids or Solids to Form Monolayers," *J. Chem. Physics*, **9**, 552- 568 (1941).

22) Ross, S., "Mechanisms of Foam Stabilization and Antifoaming Action," *Chem. Eng. Prog.*, **63**, No.9, 41-47 (1967).

23) Frumkin, A.N., "Wetting and Adherence of Bubbles", *Zh. Fiz. Khim.*, **12**, 337-345 (1938).

24) Derjaguin, B.V., "Theory of Capillary Condensation and Related Capillary Effects. Calculation of Spreading Action of Polymolecular Liquid Films, *Zh. Fiz. Khim.*, **14**, 137-147 (1940).

25) Churaev, N.V., "Wetting Films and Wetting", *Revue. Phys. Appl.*, **23**, 975-987 (1988).

26) Hirasaki, G.J., "Thermodynamics of Thin Films and Three-Phase Contact Regions", in Interfacial Phenomena in Petroleum Recovery, ed. Morrow, N.R., Marcel Dekker Inc., New York, Chapter 2, 23-76 (1991).

27) Derjaguin, B.V., and Obuchov, E., "Anomalien Dünner Flüssigkeitsschichten III, Ultramikrometrische Untersuchungen der Solvathüllen und Des elementaren Quellungsaktes", *Acta Physicochimica U.R.S.S.*, **5**,No.1, 1-22 (1936).

28) de Fries, A.J., "Foam Stability, Part V. Mechanism of Film Rupture," *Recueil*, **77**, 441-461 (1958).

29) Scheludko,A., Radoev, B., and Kolarov, T. "Tension of Liquid Films and Contact Angles Between Film and Bulk Liquid", *Trans. Faraday Soc.*, **64**, 2213-2220 (1968).

30) Rusanov, A.I., "Thermodynamics of Films", in Research in Surface Forces Vol.3, ed. B.V. Derjaguin, Consultants Bureau, Plenum Press, New York, 103-110 (1971).

31) Ivanov, I.B. and Toshev, B.V., "Thermodynamics of Thin Liquid Films, II Film Thickness and its Relation to the Surface Tension and Contact Angle", *Colloid and Polymer Sci.*, **253**, 593-599 (1975).

32) Ericksson, J.C. And Toshev, B.V., "Disjoining Pressure in Soap Film Thermodynamics", *Colloids and Surfaces*, **5**, 241-264 (1982).

33) De Feijter, J.A., Rijnbout, J.B., and Vrij, A., "Contact Angles in Thin Liquid Films, I. Thermodynamic Description," *J. Coll. Interface Sci.*, **64**, No. 2, 258-268 (1978).

34) Ivanov, I.B., and Kralchevsky, P.A., "Mechanics and Thermodynamics of Curved Thin Films," in Thin Liquid Films - Fundamentals and Applications, ed. Ivanov, I.B., Marcel Dekker Inc., New York, Chapter 11, 767-827 (1988).

35) Toshev, B.V., and Platikanov, D., "Disjoining Pressure, Contact Angles and Line Tension in Free Thin Liquid Films", *Advances in Colloid and Interface Science*, **40**, 157-189 (1992).

36) Ivanov, I.B., Toshev, B.V., and Radoev, B.P., "On the Thermodynamics of Contact Angles, Line Tension and Wetting Phenomena", in Wetting Spreading and Adhesion, ed. Padday, J.F., Academic Press, 37- 60 (1978).

37) Fagan, M.E., "The Stability of Foam and Pseudoemulsion Films and Foam Flow in Glass Beadpacks," M.S. Thesis, University of California, Berkeley (1992).

38) Bergeron, V., "Forces and Structure in Surfactant-Laden Thin-Liquid Films," Ph.D. Thesis, University of California, Berkeley (1993).

39) Khatib, Z.I., Hirasaki, G.J., and Falls, A.H., "Effects of Capillary Pressure on Coalescence and Phase Mobilities in Foams Flowing Through Porous Media", *SPERE*, **3**, No. 3, 919-926 (1988).

40) Aronson, A.S., Bergeron, V., Fagan, M.E., and Radke, C.J., "The Influence of Disjoining Pressure on Foam Stability and Flow in Porous Media," *Colloids and Surfaces*, submitted August, 1992.

41) Garrett, P.R., " The Effect of Polytetrafluoroethylene Particles on the Foam Ability of Aqueous Syrfactant Solutions", *J. Colloid Int. Sci.*, **69**, No.1, 107-121 (1979).

42) Harrold, S.P., "Purification of Sodium Dodecyl Sulfate," *J. Colloid Sci.*, **15**, 280-282 (1960).

43) Falls, A.H., Musters, J.J., and Ratulowski, J., "The Apparent Viscosity of Foams in Homogeneous Beadpacks," *SPERE*, Vol.4, No. 2, 155-164 (1989).

44) Mysels K.J., and Jones, M.N., "Direct Measurement of the Variation of Double-Layer Repulsion with Distance", *Discuss. Faraday Soc.*, **42**, 42-50 (1966).

45) Exerowa, D. and Scheludko, A., "Porous Plate Method for Studying Microscopic Foam and Emulsion Films", Chimie Physique, **24**, No.1, 47-50 (1971).

46) Scheludko, A. and Platikanov, D., "Untersuchung dunner flussiger Schichten auf Quecksicber", Kolloid. Z. 175, 150-158 (1961).

47) Bergeron, V. and Radke, C.J., "Equilibrium Measurements of Oscillatory Disjoining Pressures in Aqueous Foam Films," *Langmuir*, **8**, 3020-3026 (1992).

48) Duyvis, E. M., " The Equilibrium Thickness of Free Liquid Films," Thesis, Utrecht (1962).

Table 1. Chemical formulas of surfactants and oils.

Sodium Dodecyl Sulfate $\qquad$ $H(CH_2)_{12} O SO_3^- \quad Na^+$

Zonyl FSK $\qquad$ $F(CF_2CF_2)_{3-8}CH_2CH(OCOCH_3)CH_2N^+(CH_3)_2CH_2CO_2^-$

Dodecane $\qquad$ $C_{12}H_{26}$

Tetralin $\qquad$ $C_{10}H_{12}$
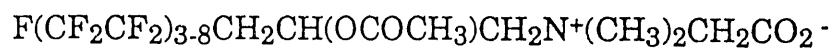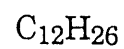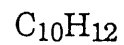
Table 2. Steady-state pressure gradients, residual oil saturations, and generalized entering coefficients.

System	$|\Delta P|/L$ (MPa/m)	S_{or} (%)	$E^g_{o/w}$ (mN/m)
SDS	29	-	
SDS (equil w/ dodecane)	6.1	-	
SDS (residual dodecane)	0.12	25	-
SDS (equil w/ tetralin)	>33	-	
SDS (residual tetralin)	0.70	10	-
SDS+NaCl	20	-	
SDS+NaCl (residual tetralin)	20	20	-0.01
Zonyl FSK	19	-	
Zonyl FSK (residual dodecane)	22	29	-0.02

Table 3. Surface and interfacial tensions, and classical entering and spreading coefficients.*

System	σ_{wg}	σ_{ow}	σ_{og} (mN/m)	$E_{o/w}$	$S_{o/w}$
SDS / Dodecane	37.8	8.9	24.3	22.4	4.6
SDS / Tetralin	34.5	4.1	35.3	3.3	-4.9
Zonyl FSK / Dodecane	15.0	9.7	24.9	-0.2	-19.6
SDS + NaCl / Tetralin	29.4	1.8	35.5	-4.3	-7.9

* Tension values, by the drop-weight method, are accurate to ± 0.5 mN/m, and entering and spreading coefficients are accurate to ± 0.9 mN/m. Systems were equilibrated at least 2 days prior to measurements. Surfactant concentrations are 0.5 active wt% and salt concentrations are 0.83 wt%.

Table 4. The lamella number and the degree of stability of flowing foam to residual oil in glass beadpacks.

System	Λ*	Stability to residual oil**
SDS / Dodecane	0.64	low
SDS / Tetralin	1.2	low
Zonyl FSK / Dodecane	0.23	high
SDS + NaCl / Tetralin	2.5	high

* $\Lambda = 0.15 \, (\sigma_{wg}/\sigma_{ow})$
** from Table 2.

Figure Captions

Figure 1. A schematic of foam flowing through a porous medium containing oil.

Figure 2. A schematic illustrating the analogy between water spreading over oil and oil entering through water. In each case the same three-phase boundary occurs.
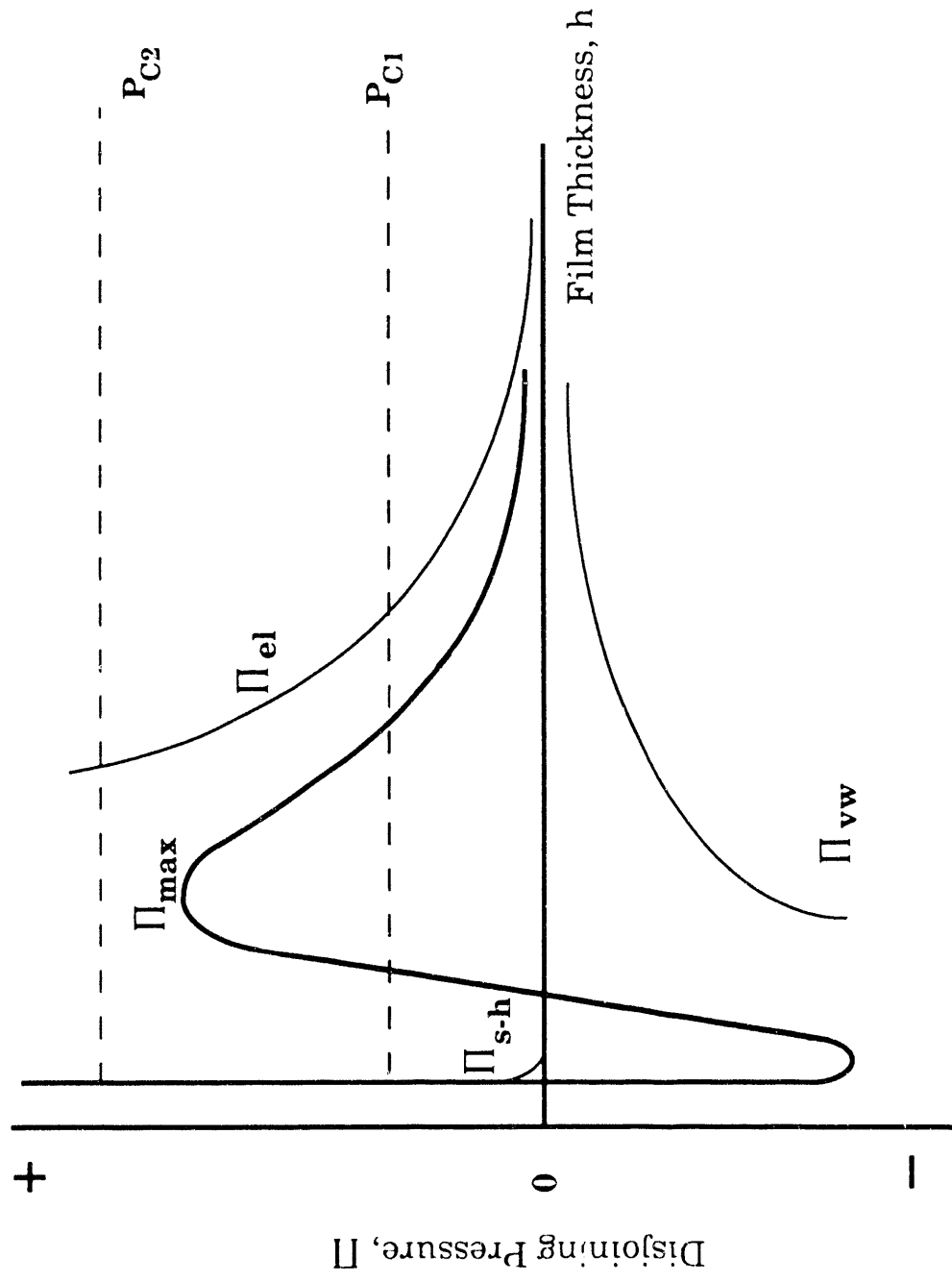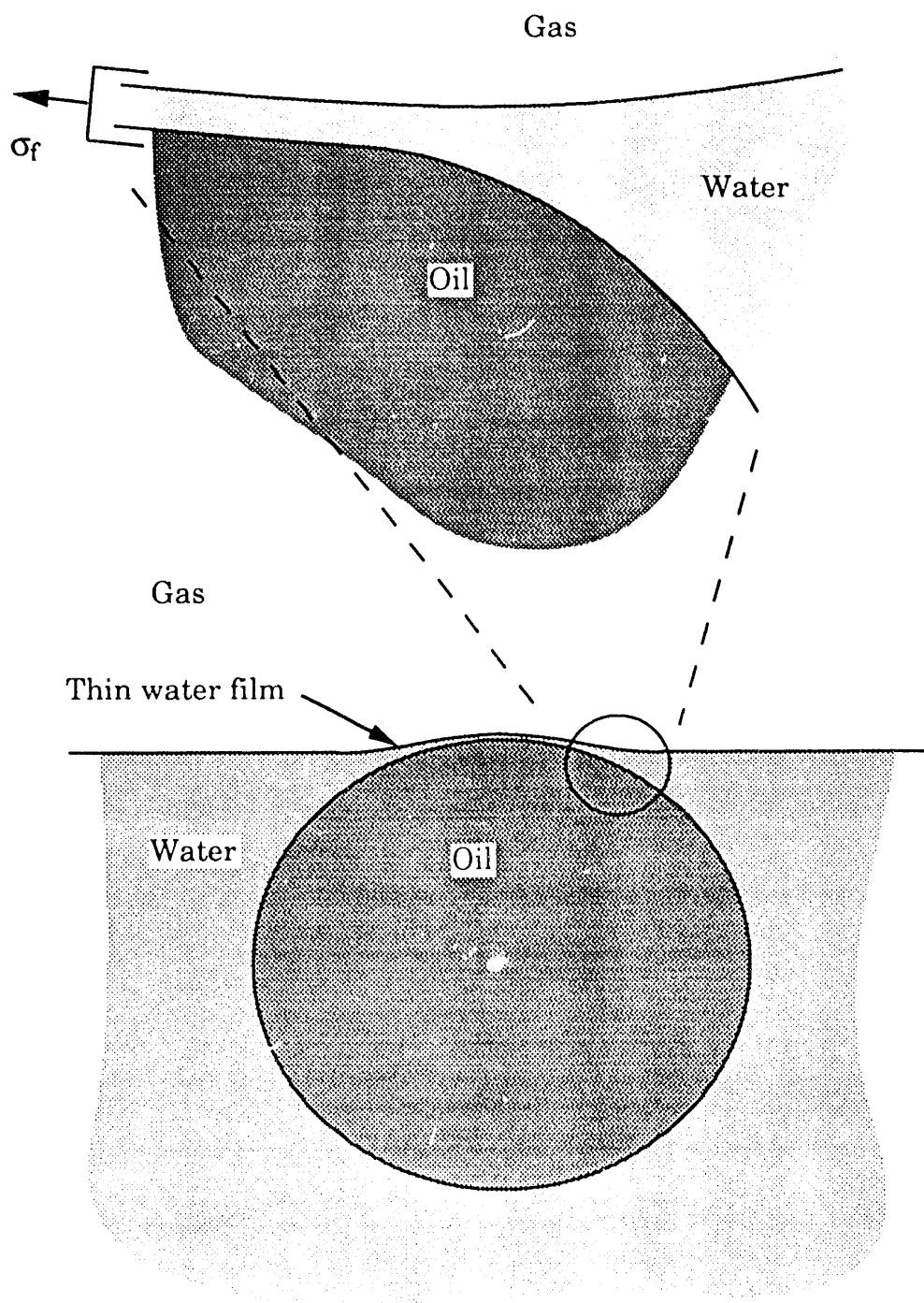
Figure 3. A typical disjoining pressure isotherm.

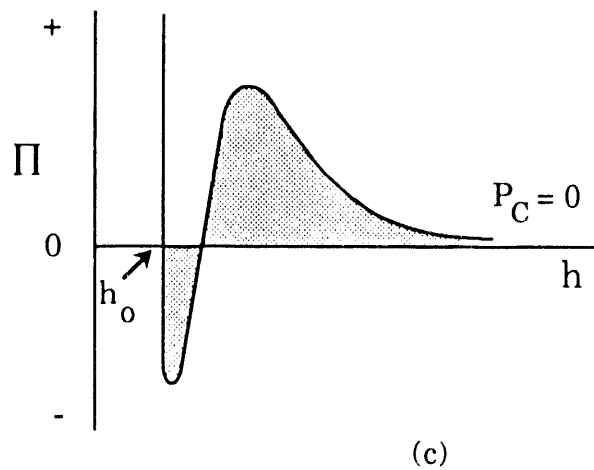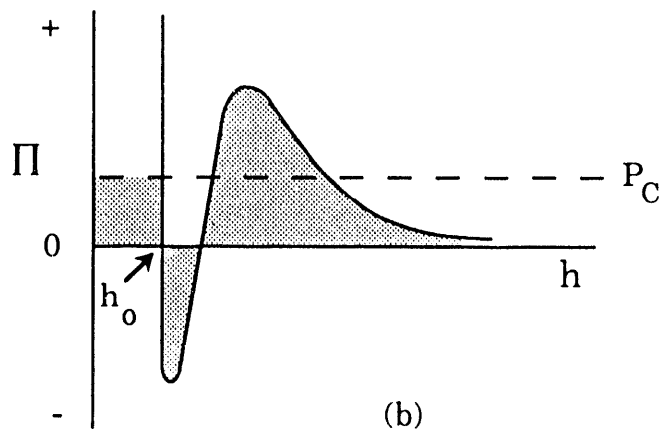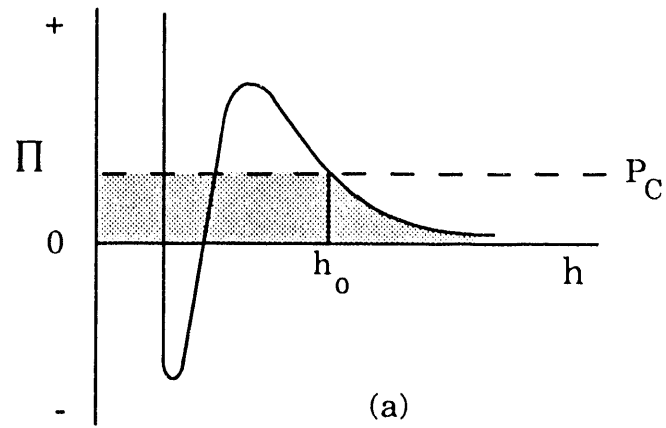Figure 4. A schematic of oil entering a water-gas interface through a thin water film.

Figure 5. Illustrations of the generalized (a,b) and classical (c) definition of the entering coefficients for a small negative well.
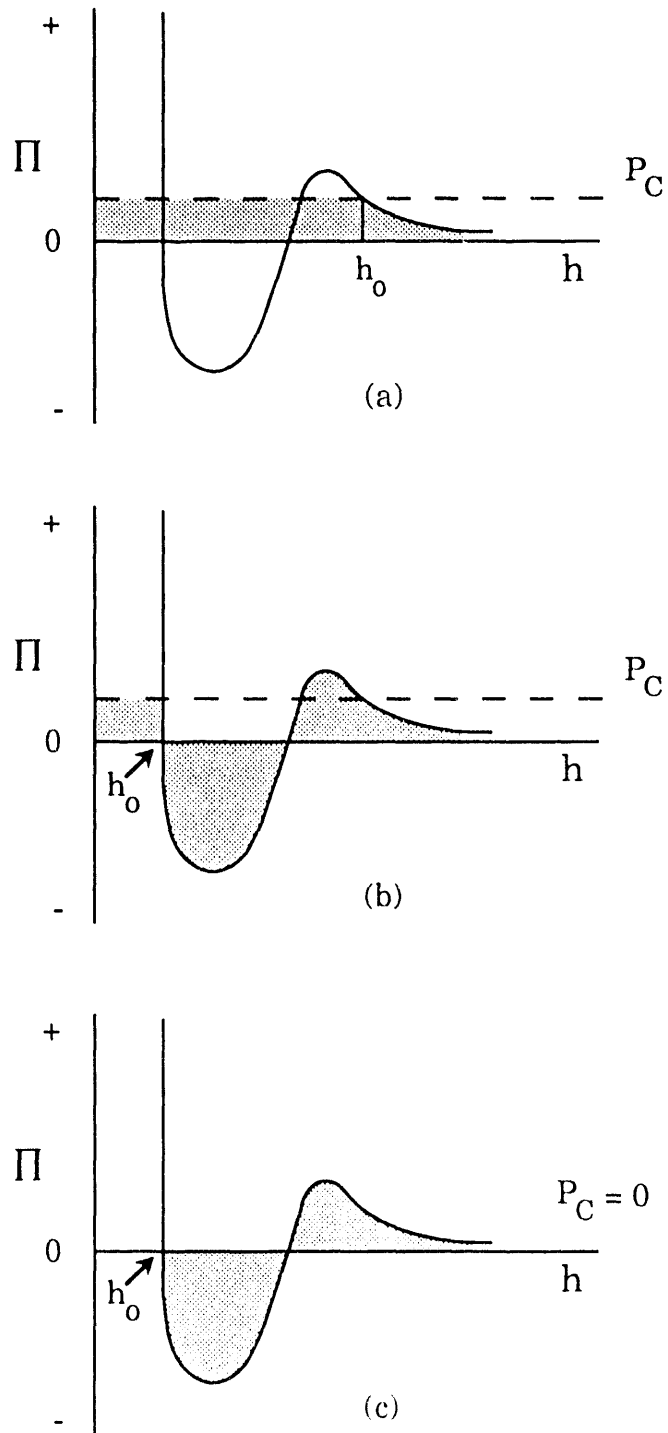
Figure 6. Illustrations of the generalized (a,b) and classical (c) definition of the entering coefficients with a large negative well.
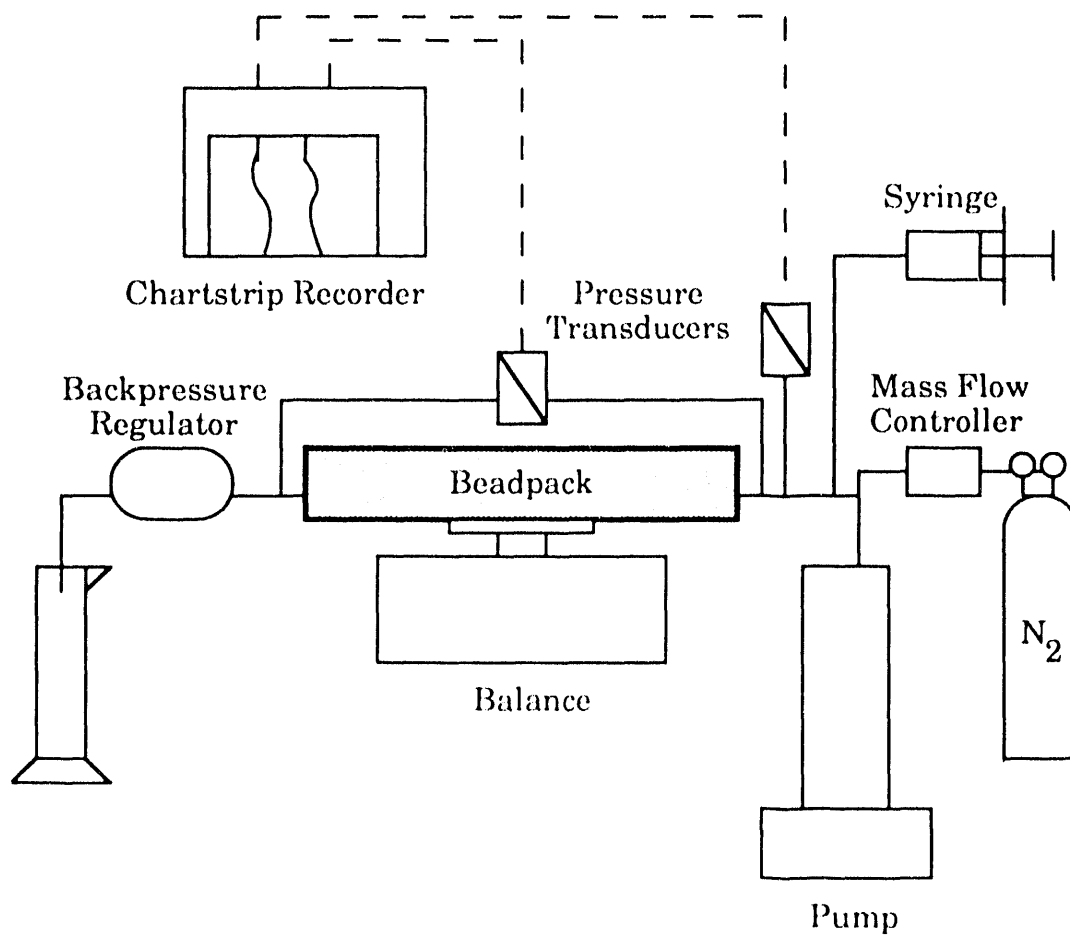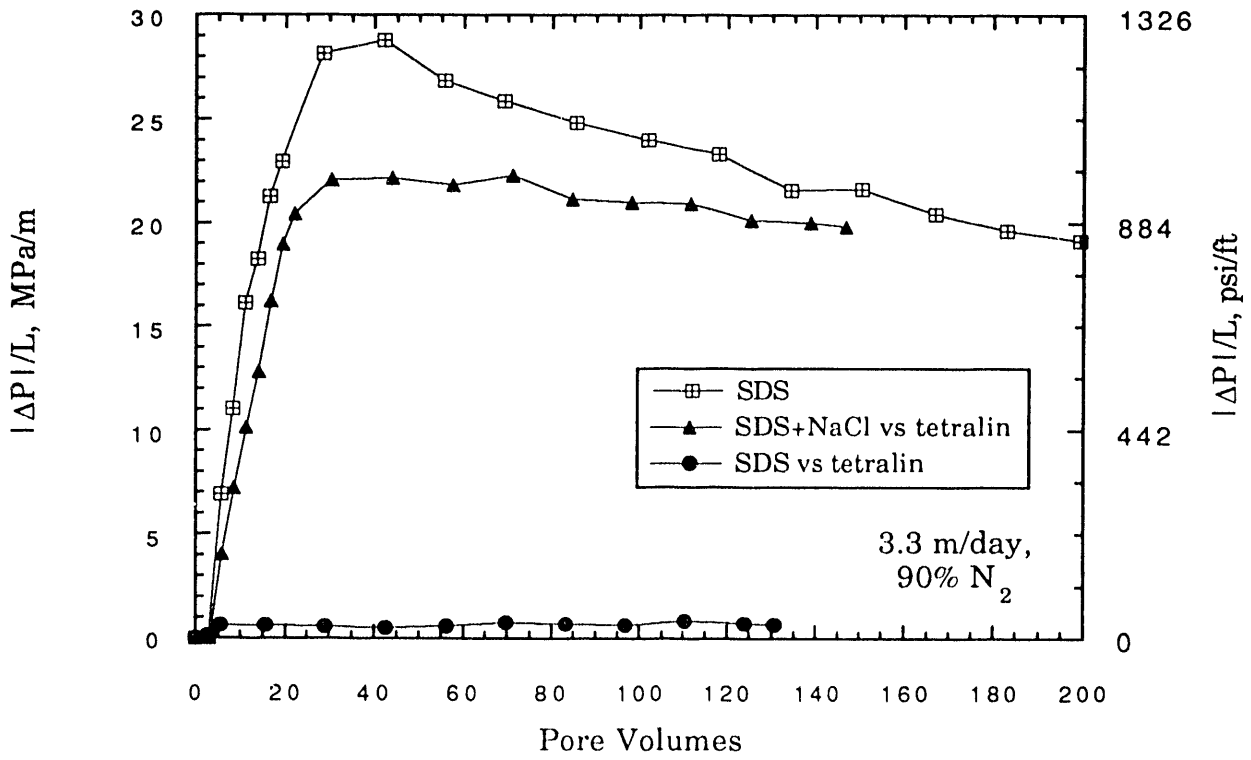
Figure 7. Schematic of the foam-flow apparatus.

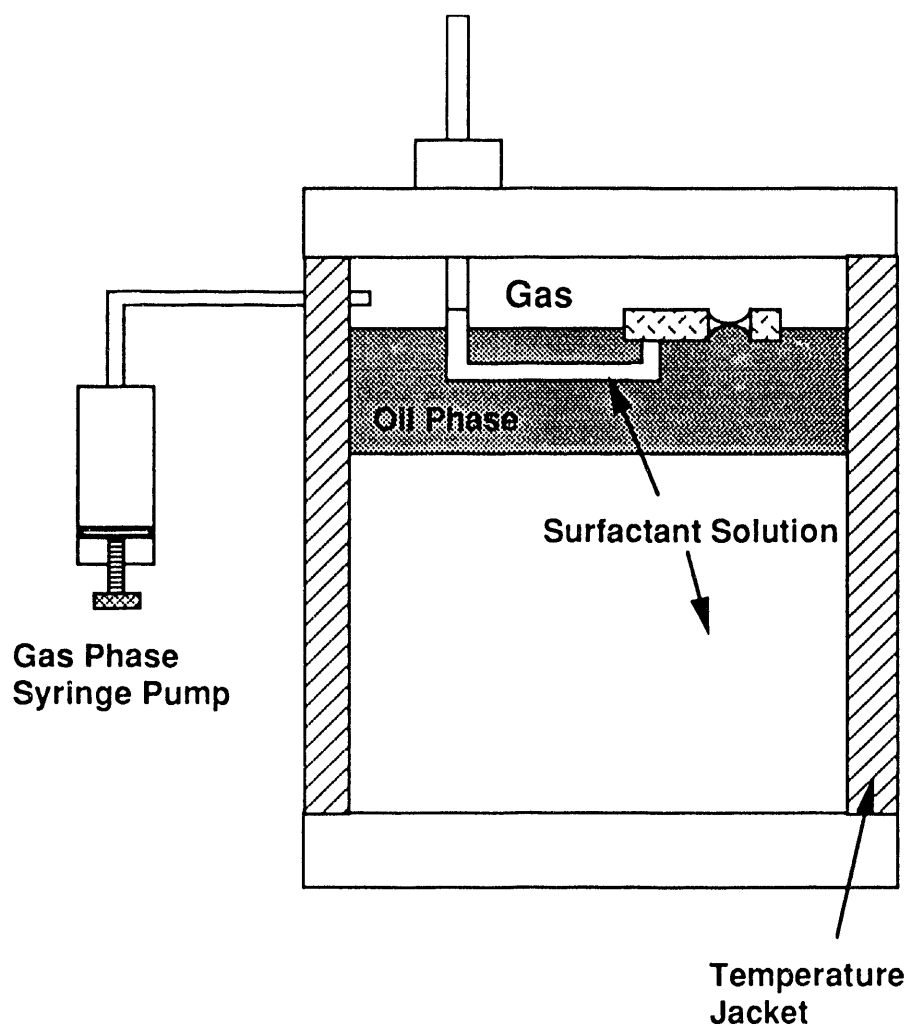Figure 8. Pressure gradient versus pore volumes for SDS/tetralin systems.

Figure 9. Disjoining pressure cell for both foam and pseudoemulsion films.

Figure 10. Foam and pseudoemulsion film (p-film) disjoining pressure isotherms and steady pressure gradients with and without residual oil for SDS/dodecane.

Figure 11. Foam and pseudoemulsion film (p-film) disjoining pressure isotherms and steady pressure gradients for SDS/tetralin.

Figure 12. Foam and pseudoemulsion film (p-film) disjoining pressure isotherms and steady pressure gradient for Zonyl FSK/dodecane.

Figure 13. Foam and pseudoemulsion film (p-film) disjoining pressure isotherms and steady pressure gradient for SDS+NaCl/tetralin.

Figure 14. Foam disjoining pressures for various SDS and SDS+NaCl solutions with and without oil equilibration.

Figure 1. A schematic of foam flowing through a porous medium containing oil.

Figure 2. A schematic illustrating the analogy between water spreading over oil and oil entering through water. In each case the same three-phase boundary occurs.

Figure 3. A typical disjoining pressure isotherm.

Gas

σ_f

Water

Oil

Gas

Thin water film

Water

Oil

Figure 4. A schematic of oil entering a water-gas interface
through a thin water film.

Figure 5. Illustrations of the generalized (a,b) and classical (c) definition of the entering coefficients for a small negative well.

Figure 6. Illustrations of the generalized (a,b) and classical (c) entering coefficients for an isotherm with a large negative well.

Figure 7. Schematic of the foam-flow apparatus.

Figure 8. Pressure gradient versus pore volumes for SDS /tetralin systems.

Gas Phase Syringe Pump

Gas

Oil Phase

Surfactant Solution

Temperature Jacket

Figure 9. Disjoining pressure cell for both foam and pseudoemulsion films.

Figure 10. Foam and pseudoemulsion film (p-film) disjoining pressure isotherms and steady pressure gradients with and without residual oil for SDS/dodecane.

Figure 11. Foam and pseudoemulsion film (p-film) disjoining pressure isotherms and steady pressure gradients for SDS/tetralin.
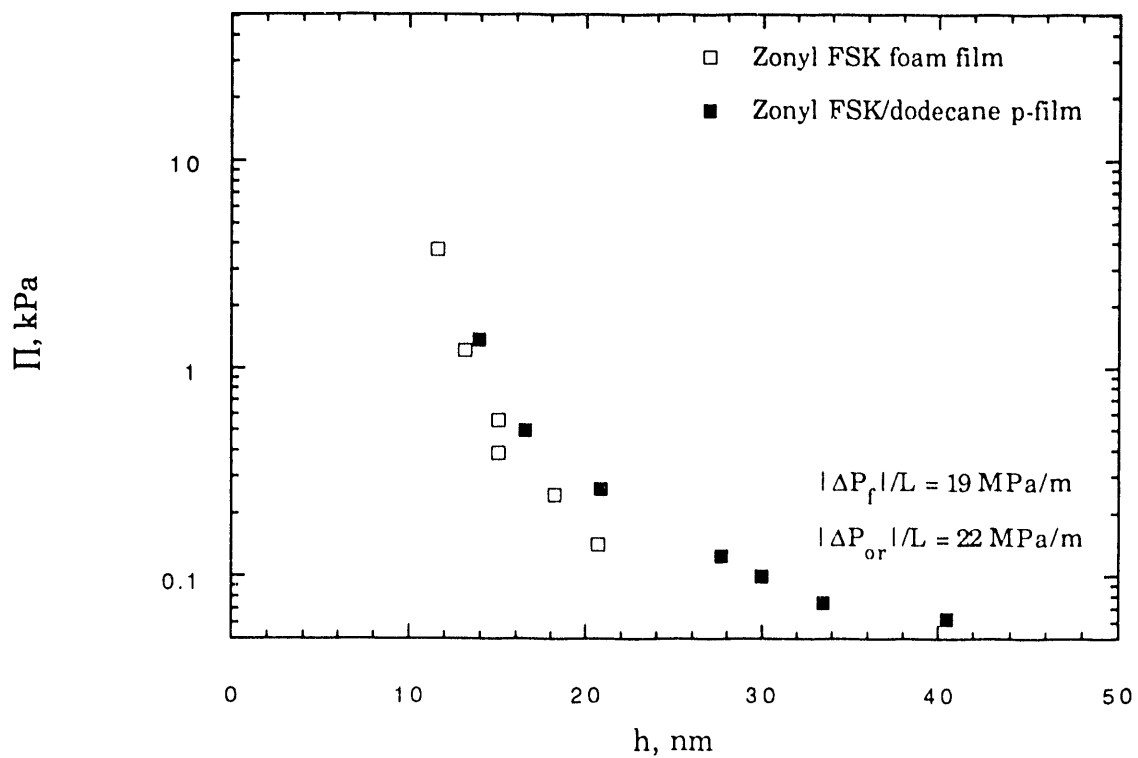
Figure 12. Foam and pseudoemulsion film (p-film) disjoining pressure isotherms and steady pressure gradient for Zonyl FSK/dodecane.
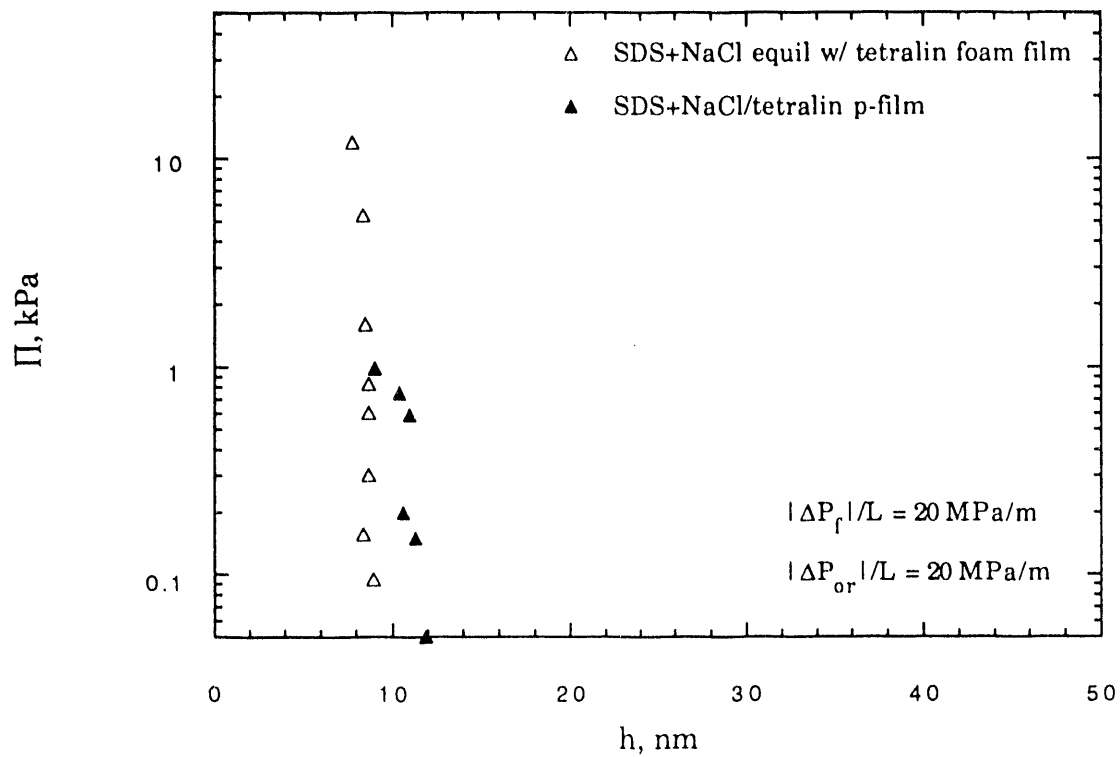
Figure 13. Foam and pseudoemulsion film (p-film) disjoining pressure isotherms and steady pressure gradient for SDS+NaCl/tetralin.
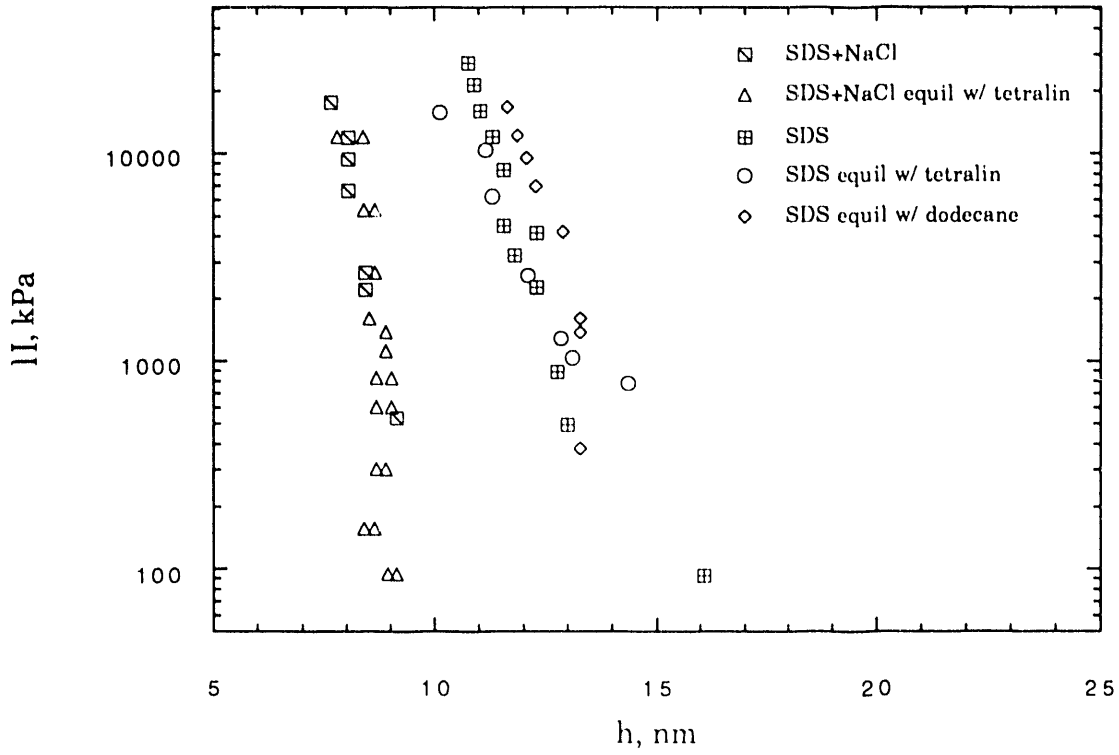
Figure 14. Foam disjoining pressures for various SDS and SDS+NaCl solutions with and without oil equilibration.

END

DATE
FILMED
12/16/93